# *In vitro* bioactivity of biphasic calcium phosphate silicate glass-ceramic in CaO-SiO$_2$-P$_2$O$_5$ system

Lachezar Radev[1,*], Vladimir Hristov[1], Irena Michailova[1], Maria Helena V. Fernandes[2], Isabel Miranda M. Salvado[2]

[1]*University of Chemical Technology and Metallurgy, Sofia, Bulgaria*
[2]*University of Aveiro and CICECO, Aveiro, Portugal*

## Abstract

*The main purpose of the paper is the evaluation of the influence of chemical composition of the gel of the synthesized 15CaO·0.5P$_2$O$_5$·6SiO$_2$ glass-ceramic on the structure, crystallization behaviour and in vitro bioactivity in static conditions for different periods of time - 3, 9 and 30 days in 1.5SBF. The obtained glass-ceramic was synthesized via polystep sol-gel technique. The structure of the prepared and the one thermally treated at 1200°C for 2 h powder was studied by XRD, $^{29}$Si MAS NMR, FTIR and SEM.*

*Keywords: calcium phosphate silicate, sol-gel, in vitro bioactivity*

## I. Introduction

Glasses [1–5] and glass-ceramic materials [6–20] based on CaO-SiO$_2$-P$_2$O$_5$ system constitute a very important group of materials that have found wide application in medicine as bone implants. These materials are able to bind with bone in an organism through the formation of carbonate containing hydroxyapatite (CO$_3$-HA) on the implant surface. Since the discovery of Bioglass (45S5) by Hench et al. [21], which had proved its favourable futures on the formation of new bone tissue at the implants site, several others glass-ceramic compositions have been attempted aiming at better suit for the bone related surgical operations. In recent years, it has also been reported that some glass-ceramics in the CaO-SiO$_2$-P$_2$O$_5$ system, containing apatite and wollastonite phases can be produced through sintering and subsequent crystallization of glass powders [7,9–11,14,22].

Analyses of the chemical and phase composition of glass-ceramic materials in the CaO-SiO$_2$-P$_2$O$_5$ system, obtained by different research groups can be summarized in Table 1.

The effect of compositional changes on the *in vitro* [7–9,20,22,23], *in vivo* [6,10,17–19] bioactivity and

other properties [11–16] have also been investigated. Margussian et al. [7] found that after one month immersion in SBF the hydroxyapatite (HA) layer can be formed on the glass-ceramic surface. They also concluded that the decrease of P$_2$O$_5$, in coincidence with [9,20], enhanced the bioactivity. Salinas et al. [8] studied that after chemical treatment of the prepared glass-ceramics with 1 M HCl, the *in vitro* studies showed the formation of an apatite-like layer covering certain areas of the material surface. In this context Pietl et al. [9] postulated that the CO$_3$HA can be formed on the glass-ceramic surface. On the base of these results, they concluded that the CO$_3$HA layer formation of these compositions in *in vitro* tests is much faster than in commercial bioactive materials such as synthetic hydroxyapatite ceramic, A/W glass-ceramic, Ceravital and Bioverit, for which the onset time usually takes at least seven days. Radev et al. [22] observed that the synthesized ceramic material with chemical composition 15CaO·P$_2$O$_5$·6SiO$_2$ demonstrates *in vitro* bioactivity in 1.5 SBF. The observed CO$_3$HA layer had a "flower-like" morphology. Radev et al. [23] also investigated that CaO-SiO$_2$-P$_2$O$_5$ glass-ceramics doped with MgO has shown *in vitro* bioactivity. They observed two types of morphologies of CO$_3$HA layer on the prepared samples - longitudinal dendrite arms and irregular assemblies of particles.

* Corresponding author: tel: +35 92 816 3280
fax: +35 92 868 5488, e-mail: *l_radev@abv.bg*

**Table 1. Chemical composition of the glass-ceramic materials, based on CaO-SiO$_2$-P$_2$O$_5$ system, obtained by different research groups**

| Authors | Chemical composition of the synthesized glass-ceramics | Phase composition | Ref. |
|---|---|---|---|
| L. Meseguer-Olmo | 55SiO$_2$-41CaO-4P$_2$O$_5$ (mol%) | $\alpha$-CaSiO$_3$, $\beta$-CaSiO$_3$, Ca$_3$(PO$_4$)$_2$, SiO$_2$ | [10] |
| L.Hench | 45SiO$_2$-24.5CaO-24.5Na$_2$O-6P$_2$O$_5$ (mol%) | not specified | [21] |
| A.Balamurugan | 55 SiO$_2$-26CaO-13MgO-6P$_2$O$_5$ (mol%) | (Ca,Mg)$_3$(PO$_4$)$_2$, Mg$_2$SiO$_4$ | [6] |
| O. Peitl | 1.5Na$_2$O-1.5CaO-3SiO$_2$ - 0,2,4 and 6 P$_2$O$_5$ | Ca$_{10}$(PO$_4$)$_6$(OH), CaSiO$_3$ | [9] |
| V.K. Marghussian | 44.9CaO-34.2SiO$_2$-16.3P$_2$O$_5$-4.6MgO<br>44.9CaO-37.2SiO$_2$-13.3P$_2$O$_5$-4.6MgO<br>44.9CaO-40.2SiO$_2$-10.3P$_2$O$_5$-4.6MgO<br>44.9CaO-43.2SiO$_2$-7.3P$_2$O$_5$-4.6MgO (wt.%) | Ca$_{10}$(PO$_4$)$_6$(OH),<br>CaSiO$_3$,<br>Ca$_3$(PO$_4$)$_2$ | [7] |
| H.-L. Ren | 47CaO-34.5SiO$_2$-14P$_2$O$_5$-1B$_2$O$_3$-1.5ZnO-2MgO;<br>47CaO-34.5SiO$_2$-14P$_2$O$_5$-1B$_2$O$_3$-2.5ZnO-1MgO | $\beta$-CaSiO$_3$,<br>Ca$_{10}$(PO$_4$)O$_6$ | [11] |
| H. Aguiar | Na$_2$O-MgO-CaO-P$_2$O$_5$-SiO$_2$ | not specified | [12] |
| A. Salinas | 40CaO-34.5SiO$_2$-16.5P$_2$O$_5$-8.5MgO-0.5CaF$_2$ (wt.%) | Ca$_{10}$(PO$_4$)$_6$(OH)$_2$, MgCaSi$_2$O$_6$,<br>Mg$_2$(PO$_4$)(OH,F,O),<br>Ca$_2$MgSi$_2$O$_7$ | [8] |
| R.K. Singh | 41CaO-(52-x)SiO$_2$-4P$_2$O$_5$-xFe$_2$O$_3$-3Na$_2$O<br>(x = 0, 2, 4, 6, 8, 10 mol%) | Ca$_{10}$(PO$_4$)$_6$(OH)$_2$, Fe$_3$O$_4$,<br>CaSiO$_3$ | [14] |
| D. Eniu | xFe$_2$O$_3$ -45(3.34CaO-P$_2$O$_5$)(55-x)SiO$_2$ | not specified | [15] |
| K. Sharma | 25SiO$_2$-50CaO-15P$_2$O$_5$-(10-x)Fe$_2$O$_3$-xZnO<br>(x = 0, 2, 5 mol%) | Ca$_3$(PO$_4$)$_2$, Fe$_3$O$_4$,<br>ZnFe$_2$O$_4$ | [13] |
| B. Yu | 30CaO-25P$_2$O$_5$-40SiO$_2$-5MgO-5Al$_2$O$_3$<br>30CaO-25P$_2$O$_5$-39SiO$_2$-5MgO-5Al$_2$O$_3$-1ZrO$_2$<br>29CaO-25P$_2$O$_5$-38SiO$_2$-5MgO-5Al$_2$O$_3$-3ZrO$_2$<br>29CaO-24P$_2$O$_5$-38SiO$_2$-5MgO-5Al$_2$O$_3$-5ZrO$_2$<br>29CaO-24P$_2$O$_5$-38SiO$_2$-4MgO-4Al$_2$O$_3$-7ZrO$_2$ (wt.%) | Ca$_{10}$(PO$_4$)$_6$(OH)$_2$,<br>CaSiO$_3$,<br>K[AlSi$_2$O$_6$] | [16] |
| E. Leonardi | P$_2$O$_5$-SiO$_2$-CaO-MgO-Na$_2$O-K$_2$O | Na$_2$Mg(PO$_4$)$_3$, Ca$_2$P$_2$O$_7$ | [17] |
| G.Li | Doping Mg ferrite to wollastonite-fluorapatite-containing glass-ceramics | CaSiO$_3$,Ca$_2$MgSi$_2$O$_7$, Ca$_5$(PO$_4$)$_3$F,<br>Fe$_2$MgO$_4$ | [18] |
| E. Verné | 57SiO$_2$-3Al$_2$O$_3$-34CaO-6Na$_2$O<br>47.5SiO$_2$-2.5P$_2$O$_5$-30CaO-10K$_2$O-10Na$_2$O<br>45SiO$_2$-3P$_2$O$_5$-7MgO-26CaO-4K$_2$O-15Na$_2$O | not specified | [19] |
| Z. Hong | 66SiO$_2$-27CaO-7P$_2$O$_5$ (mol%) | not specified | [20] |
| L. Radev | 62.6CaO-26.8SiO$_2$-10.6P$_2$O$_5$ (wt.%) | Ca$_{15}$(PO$_4$)$_2$(SiO$_4$)$_6$,<br>$\alpha$-CaSiO$_3$, $\beta$-CaSiO$_3$ | [22] |
| L. Radev | 46.7CaO-34.2SiO$_2$-15.9P$_2$O$_5$-2.9MgO (wt.%) | Ca$_2$MgSi$_2$O$_7$, Ca$_{10}$(PO$_4$)$_6$(OH)$_2$ | [23] |
| L. Radev | 62.5CaO-21.7SiO$_2$-9.9P$_2$O$_5$-5.9MgO (wt.%) | (Ca,Mg)$_3$(PO$_4$)$_2$, Ca$_5$(PO$_4$)$_2$SiO$_4$ | [23] |

In this paper, we investigated the influence of composition of the prepared glass-ceramic with chemical composition $15CaO \cdot 0.5P_2O_5 \cdot 6SiO_2$ on the structure, crystallization behaviour and *in vitro* bioactivity in static conditions for different periods of time.

## II. Experimental

### 2.1 The *synthesis of the ceramic sample*

The ceramic material in the $CaO-SiO_2-P_2O_5$ system has been synthesized via polystep sol-gel method. The chemical composition of the obtained sample is described as 66.1 CaO, 28.3 $SiO_2$ and 5.6 $P_2O_5$ (wt.%).

The procedure for the synthesis of the ceramic material with chemical composition of the gel $15CaO \cdot 0.5P_2O_5 \cdot 6SiO_2$ is similar to this detail documented in ref. 22. The obtained mixed (calcium phosphate-$SiO_2$) sol was gelated at 120°C for 12 hours and thermally treated at 1200°C for 2 hours in tubular furnace.

### 2.2 In vitro test for bioactivity in static conditions

Bioactivity of obtained ceramic materials was evaluated by examining the apatite formation on their surfaces in 1.5SBF (simulated body fluid). The 1.5SBF solution was prepared from reagents as follows: NaCl = 11.9925 g, $NaHCO_3$ = 0.5295 g, KCl = 0.3360 g, $K_2HPO_4 \cdot 3H_2O$ = 0.3420 g, $MgCl_2 \cdot 6H_2O$ = 0.4575 g, $CaCl_2 \cdot 2H_2O$ = 0.5520 g, $Na_2SO_4$ = 0.1065 g, and buffering at pH 7.4 at 36.5°C with *TRIS*=9.0075 g and 1M HCl in distilled water. The synthesized ceramic powder was pressed at 50 MPa with PVA to obtain disc specimens (12 mm diameter and 2 mm thick) and immersed in 1.5SBF at the human body temperature (36.6°C) in polyethylene bottles in static conditions for 3, 9 and 30 days. A few drops of 0.5% sodium azide ($NaN_3$) was added to the 1.5 SBF solution to inhibit the growth of bacteria [24,25]. After soaking, the specimens were removed from the fluid and gently rinsed with distillated water, and then dried at 36.6°C for 12 h.

### 2.3 Methods for analysis

The structure and in vitro bioactivity of ceramic materials was monitored by X-ray diffraction (XRD) analysis, Fourier-transform infrared (FTIR) spectroscopy and scanning electron microscopy with X-ray microanalysis (SEM/EDS).

Powder X-ray diffraction spectra were collected within the range from 10° to 80° $2\theta$ with a constant step 0.04° $2\theta$ and counting time 1 s/step on a Bruker D8 Advance diffractometer with $CuK_\alpha$ radiation and SolX detector. The spectra were evaluated with the Diffrac*plus* EVA package.

FTIR transmission spectra for the obtained hybrids were recorded by using a Bruker Tensor 27 spectrometer with scanner velocity 10 kHz. KBr pellets were prepared by mixing ~1 mg of the samples with 300 mg KBr. Transmission spectra were recorded using MCT detector, with 64 scans and 1 cm⁻¹ resolution.

SEM (Jeol, JSM-35 CF, Japan) in conjunction with EDS was used to ascertain the morphology and chemical constituents of the prepared hybrids after immersion in 1.5 SBF for 3 days at accelerating voltage of 15 kV.

²⁹Si magic-angle spinning (MAS) NMR spectra were recorded at 79.49 MHz on a 9.4 T Bruker Avance 400 spectrometer, using 408 pulses, a recycle delay of 60 s and a spinning rate of 5 kHz.

## III. Results and discussion

### 3.1 Characterization of the obtained ceramic powder before in vitro test

X-ray diffraction patterns, for the synthesized and thermally treated at 1200°C sample, are depicted in Fig. 1. XRD showed the presence of $Ca_{15}(PO_4)_2(SiO_4)_6$ (PDF 50-0905) and $Ca_2SiO_4 \cdot 0.05Ca_3(PO_4)_2$ (PDF 49-1674). The presented XRD data is in a good agreement with Mumme et al. [26].

²⁹Si MAS NMR spectroscopy in the solid state provides significant information about the different silicon species that constitute the structure formed, as well as the degree of condensation between the silicate sheets in the structure of the hybrid. The $Q^n$ notation is convenient for indicating the number of $n$ of –O-Si link-
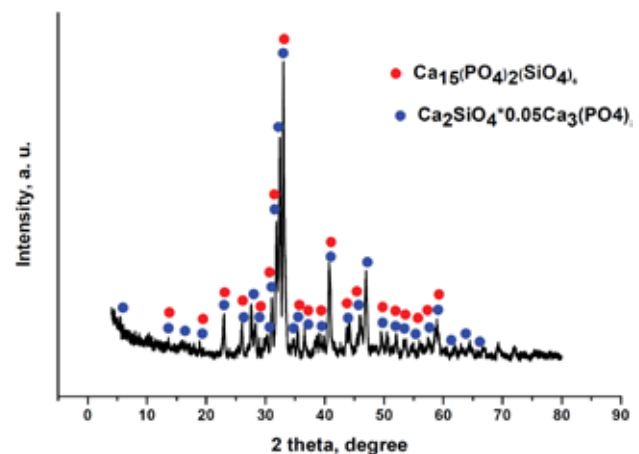


**Figure 1 XRD data for the prepared sample, treated at 1200°C for 2 h**
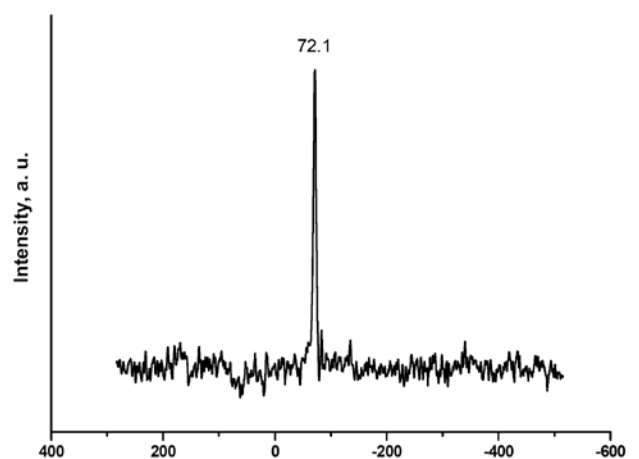


**Figure 2. ²⁹Si MAS NMR for the thermally treated at 1200°C for 2 hours glass-ceramic**
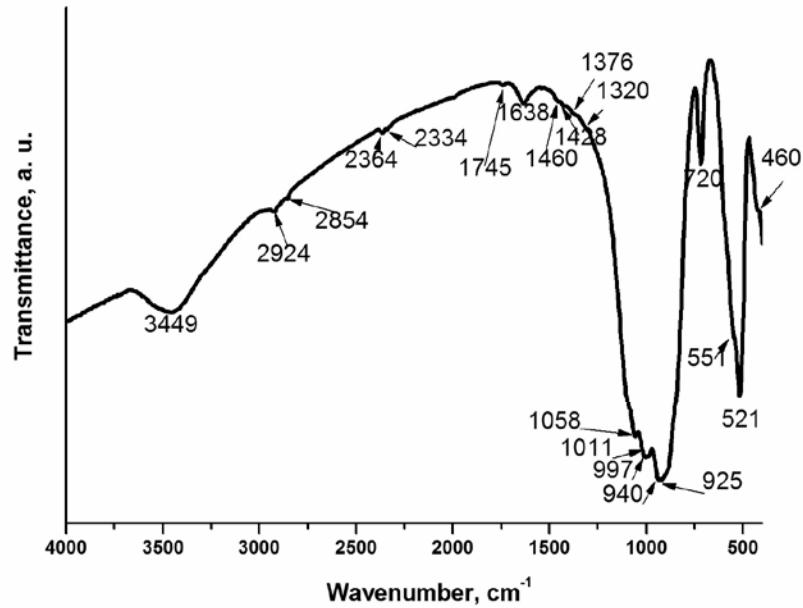
**Figure 3. FTIR spectrum for calcium phosphate silicate obtained after heating at 1200°C for 2 hours**

ages of Si atom. Fig. 2 presents $^{29}$Si MAS NMR spectra for the synthesized ceramic material after annealing at 1200°C for 2 hours. As it can be seen, in the synthesized sample there is only $Q^o$ (-72.1 ppm) silicon environments ($\equiv$Si(O-)$_4$) [27]. From the obtained result we can assume that large fraction of the Si(IV) was incorporated into the calcium phosphate lattice in the form of $Q^o$ species [28]. On the other hand, from Fig. 2 we can also see that one sharp signal located at -72.1 ppm indicates that the crystalline phases are separated from the glass according to Ren et al. [11] in MgO-CaO-SiO$_2$-P$_2$O$_5$ bioglass-ceramics.

Fig. 3 shows FTIR spectrum for the obtained sample after thermal treatment at 1200°C for 2 hours. In the presented spectrum the absorption bands of silicate groups were clearly evident. The intense band centred at 990 cm$^{-1}$ was assigned to the Si-O-Si asymmetric stretch [29], the bands at 940 and 925 cm$^{-1}$ to the Si-O symmetric stretch [29–32] and the bands at 551, 521 and 460 cm$^{-1}$ to the Si-O-Si vibrational mode of bending [29,30,33,34]. The band, centred at 521, 551, 630 and 1011 cm$^{-1}$ can be assigned to the presence of $v_3$ SiO$_4$ or $v_4$ PO$_4$ groups [30,31,35–38]. Around 720 cm$^{-1}$ in the prepared sample is the
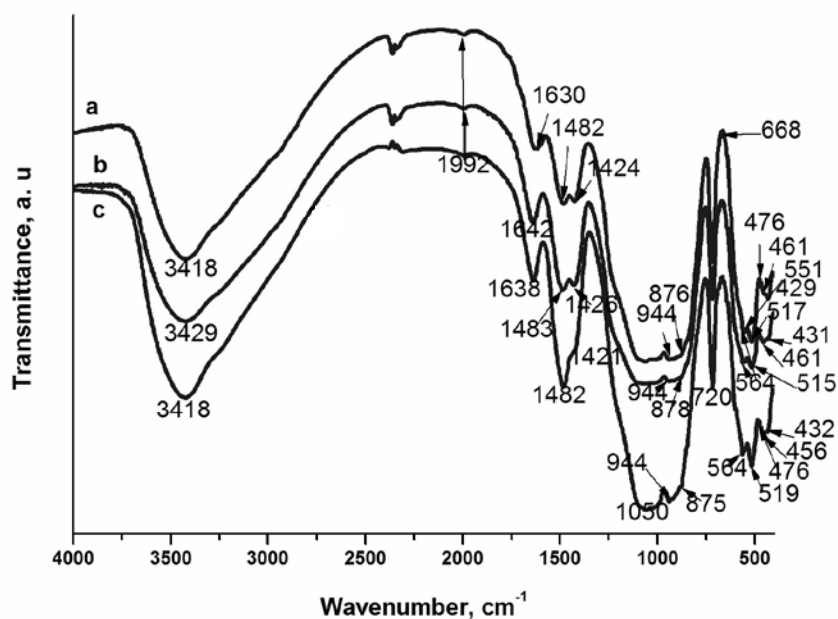


**Figure 4. FTIR spectra of the samples after *in vitro* test for bioactivity in static conditions for 3 days (a), 9 days (b) and 30 days (c)**

band due to Si-O bending vibrations [39]. The important vibrations of the $PO_4^{3-}$ can be distinguished in the three main regions: i) a sharp peak at 1058 cm⁻¹ associated with asymmetric stretching vibration [40]; ii) a weak bands at 940 and 925 cm⁻¹ corresponding to the symmetric stretching [38,40,41]; iii) two well resolved peaks at 551 and 525 cm⁻¹ assigned to the asymmetric bending modes [42–44]. In our synthesized sample, however, the characteristic bands with small intensity, posited at 1011 and 940 cm⁻¹ could be ascribed to the presence of β-tricalcium phosphate (β-TCP) in accordance with Ooi et al. [45] and de Aza et al. [46,47]. Furthermore, in keeping with Gou et al. [29] the absorption bands, posited at 997, 940 and 521 cm⁻¹, respectively could be ascribed to the presence of $Ca_2SiO_4$. The double peaks at 2364 and 2334 cm⁻¹ assigned to the O-H stretch vibration of hydrogen bonded O-H groups, together with the peak at 1638 cm⁻¹ ascribed to the O-H bending mode are evidences of the presence of adsorbed water in the prepared ceramic powder [48]. Surprisingly, as it can be seen from the presented Fig. 3, we can observe the bands, centred at 1745, 1460, 1428, 1376 and 1320 cm⁻¹. The assignments for $CO_3^{2-}$ in the prepared ceramic powder are $v_3$ (asymmetric stretching) at 1460, 1428 and 1376 cm⁻¹ and $v_2$ (bending) at 1320 cm⁻¹ [36,49–51]. The band centred at 1750 cm⁻¹ can be attributed to the presence of small amount of calcite [52]. The presence of carbonate bands is attributed to a carbonation process of the material due to the atmospheric $CO_2$ as a consequence of the high calcium content in the prepared sample. The obtained results are in a good correspondence with those, published by Martinez et al. [53] for $CaO-SiO_2$ sol-gel glasses. Moreover, the spectrum do not display a number of very weak absorption bands at 2900–2800, 1644 and 878 cm⁻¹. According to Zaki et al. [54,55] these bands are indicative for pure CaO.

Fig. 4 presents the FTIR data after immersion of the prepared ceramic in 1.5SBF for different periods of time - 3, 9 and 30 days As it can be seen, Fig. 4 shows the infrared absorption spectra of carbonate containing hydroxyapatite ($CO_3HA$) formed on the surface of the immersed samples for 3, 9 and 30 days. The $v_1$ mode of $PO_4^{3-}$ ion is represented in apatite by a very narrow band at 944 cm⁻¹ and the $v_2$ mode produces an absorption peak, centred at 476 cm⁻¹ (Fig. 4, curves a and c) and 461 cm⁻¹ (Fig. 4, curve b) [56–60]. As shown by other authors, the main absorbance signal of $PO_4^{3-}$ appears in the triply degenerate $v_3$ domain [58]. Moreover, the $v_4$ mode gives a well defined peak, posited at 564 cm⁻¹ [58,60]. The broad peak at around 1000 cm⁻¹ (1050 cm⁻¹ for all three samples) is due to both the $v_1$-$v_3$ $PO_4^{3-}$ modes and the most intense $SiO_4^{4-}$ absorption band [58–60]. The $v_2$ signal is also masked by another Si-O-Si peak, and the only well defined $PO_4^{3-}$ band
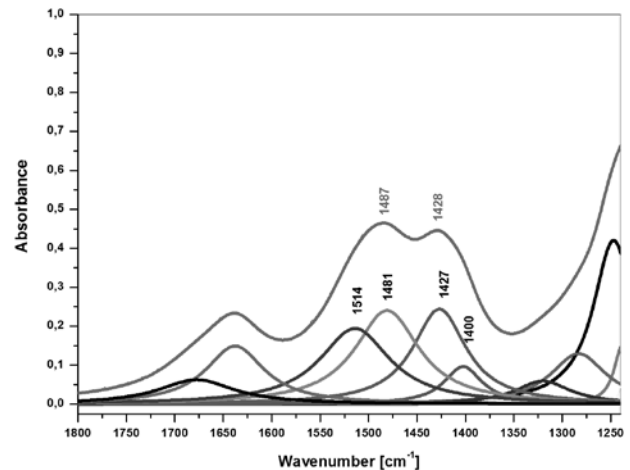


**Figure 5 Curve fitting spectra of the type of $CO_3HA$, formed on the ceramic sample after 30 days immersion in 1.5SBF**

is thus the doubly degenerate $v_4$ mode. Among the four internal vibrational modes of the free $CO_3^{2-}$ ion, only two are of importance for FTIR investigations in calcium phosphates: $v_2$ and $v_3$ [61]. In the presented FTIR spectra, the absence of the C-O absorption bands at ~710 cm⁻¹ indicates that no detectable calcite or aragonite is associated with our $CO_3HA$ over the synthesized sample after static in vitro test. This result confirms our X-ray diffraction analysis, depicted on Fig. 6. On the one hand, Feki et al. [62] postulated that the absorption band, posited at 720 cm⁻¹ could be assigned to the presence of B-substitution ($CO_3^{2-} \rightarrow PO_4^{3-}$) into hydroxyapatite lattice. On the other hand, the weak bands centred at ~876, ~1480 and ~1423 cm⁻¹ could be ascribed to the B-substitution into hydroxyapatite lattice, as already mentioned in literature [59–61,63].

The more detailed information about the type of substitution in $CO_3HA$, formed on the surface of the prepared ceramic, after 30 days immersion in 1.5SBF, was analyzed by curve fitting in the region 1850–1250 cm⁻¹ (Fig. 5). It can be seen that the bands centred at 1481, 1427 and 1400 cm⁻¹ could be ascribed to the presence of B-type carbonate substitution, i. e. part of $PO_4^{3-}$
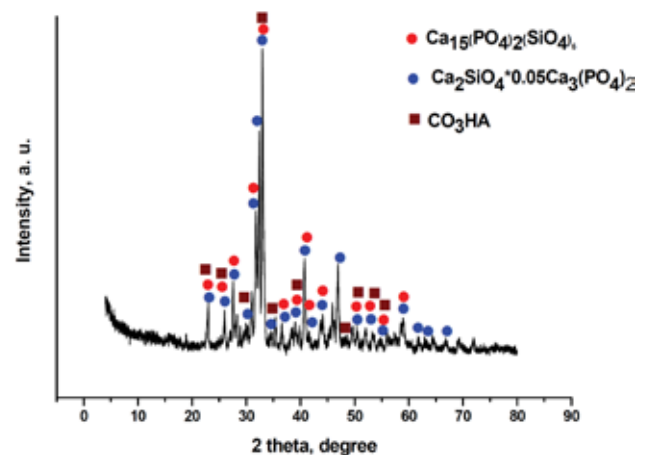


**Figure 6. XRD of the ceramic sample after immersion in 1.5SBF for 3 days in static conditions**
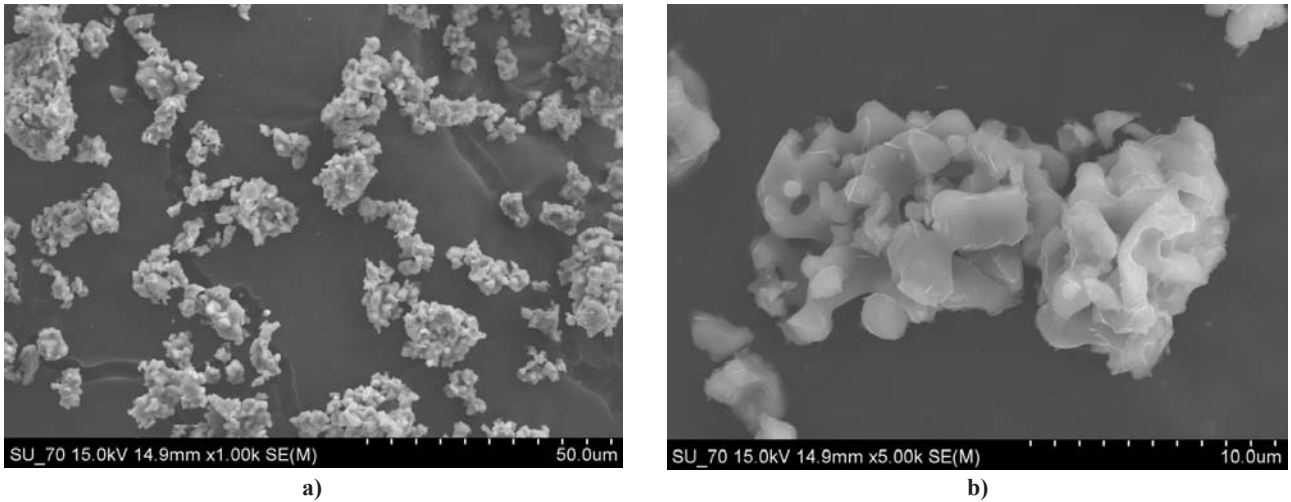
**Figure 7. SEM of the synthesized and thermally treated ceramic powder at different magnifications before *in vitro* test**

was replaced by $CO_3^{2-}$ [53,61,64–68]. As indicated earlier by Fleet et al. [69] the peak, posited at 1514 cm⁻¹ can be related to the presence of A-type substitution ($CO_3^{2-}\rightarrow OH^-$) into hydroxyapatite lattice.

XRD of the synthesized sample after 3 days immersion in 1.5SBF is given in Fig. 6. From depicted XRD patterns it can be seen that the obtained samples do not undergo drastic changes after 3 days immersion in 1.5SBF. As can be seen, the mean diffrac-

tion peaks of $CO_3HA$ (PDF 04-0697) are presented. The obtained XRD results are in accordance with presented FTIR data.

SEM of the prepared calcium phosphate silicate ceramic powder, after thermal treatment at 1200°C for 2 hours, clearly depicts (Fig. 7b) that the synthesized sample has a plate-like morphology. This morphology is characteristic for the silicon substituted apatites as denoted in [70].
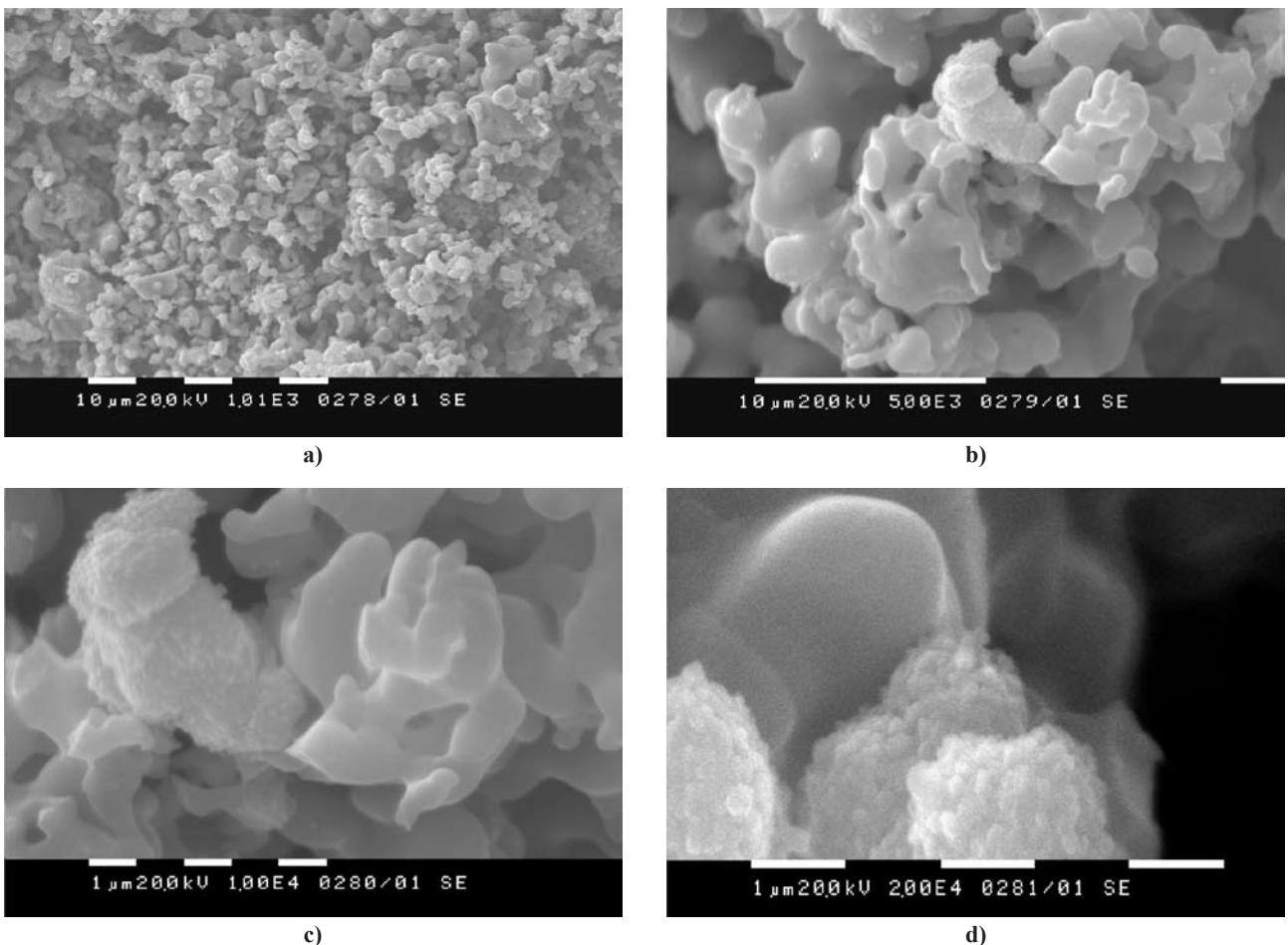


**Figure 8. SEM of the synthesized ceramic sample after 9 days immersion in 1.5SBF at different magnifications**

a)



b)



c)



d)
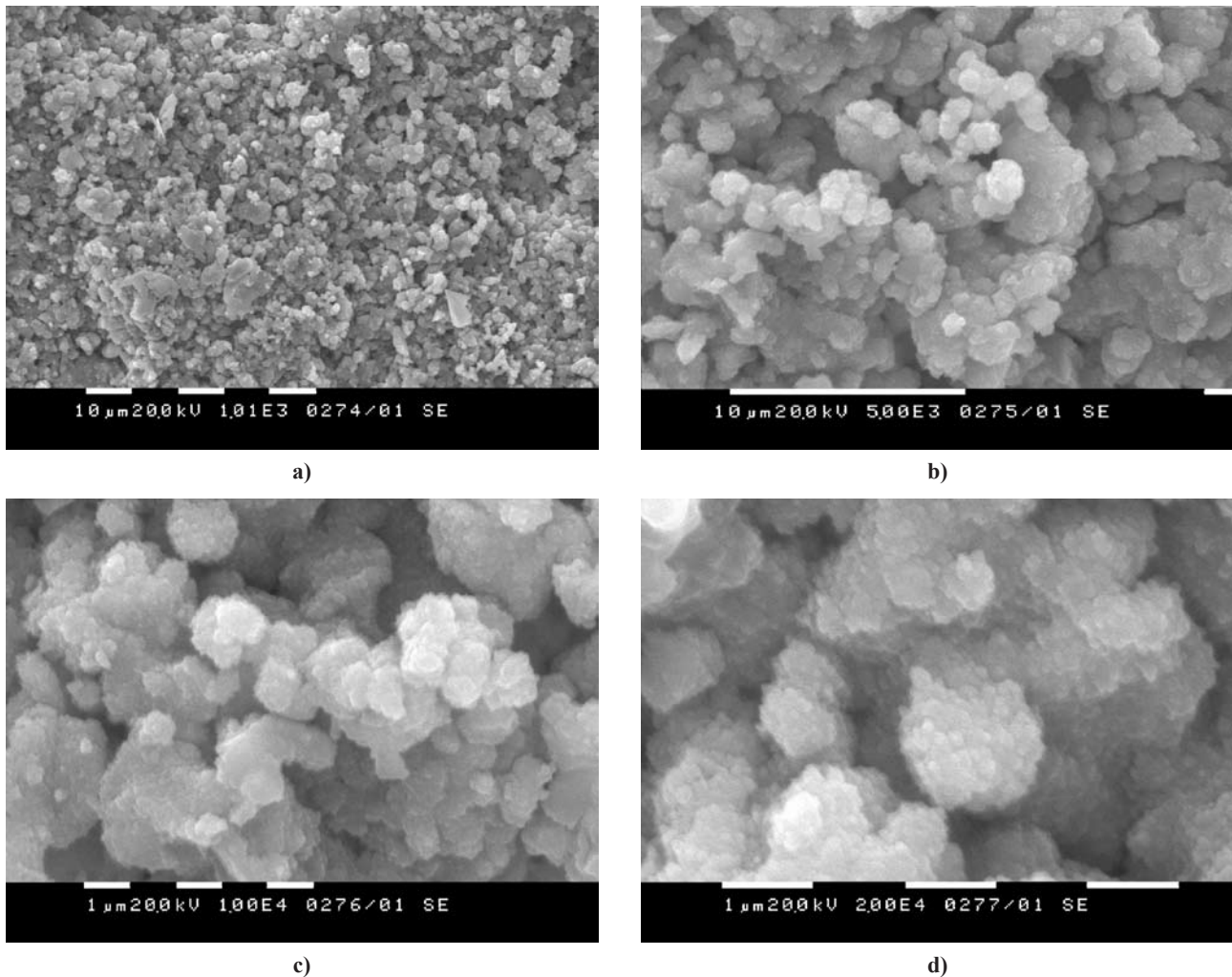
**Figure 9. SEM of the synthesized sample after 30 days immersion in 1.5SBF at different magnifications**

From the presented SEM images it can also be seen that the prepared powder has none fully densified structure. Some authors postulate that the preparation of this structure could be assigned to the presence of silica in calcium phosphate structure and the temperature of thermal treatment of dried calcium phosphate silicate gel [71].

SEM images for the samples after *in vitro* test for 9 and 30 days are given in Figs. 8 and 9. After immersion of the prepared ceramics for different periods of time, it is observed (Figs. 8a and 9a) that the surface of the immersed samples is fully covered with the particles with different morphology. When the ceramic was immersed for 9 days in 1.5-SBF in static conditions, SEM showed that on the surface are deposited some spherical particles (Fig. 8b,c). The diameters of these spheres were 1–3 µm. At low magnification (Fig. 8b), it may seem to us that the spheres had crackles on their bumpy surface. But it is not so. At high magnification (Fig. 8d) it can be seen that the big spherical particles composed of small nanospheres. The diameter of these spheres riches up to 0.2 µm. After 30 day immersion in 1.5SBF in static conditions, SEM depicts that a dense deposits cover

the entire surface of the prepared ceramic. As can be seen from Fig. 7b such deposits are not observed prior in vitro test in static conditions. At high magnification (Fig. 9c,d) we can also see that the spherical particles are accumulated on the ceramic surface. As it has been explained above, these spheres are consisted of the little spheres. These spheres have a diameter of 0.1–0.2 µm

## IV. Conclusions

A new biphasic calcium phosphate silicate ceramic material has been synthesized via polystep sol-gel method. After thermal treatment of the dried gel at 1200°C for 2 h, XRD showed the presence of two phases - $Ca_{15}(PO_4)_2(SiO_4)_6$ and $Ca_2SiO_4 \cdot 0.05Ca_3(PO_4)_2$ FTIR study confirmed XRD data. $^{29}$ SiMAS NMR indicated that the obtained material has only $Q^o$ (-72.1 ppm) silicon environments ($\equiv Si(O-)_4$). *In vitro* evaluation of bioactivity was carried out in static conditions in 1.5SBF. FTIR spectra showed that the increase in the intensity of $CO_3^{2-}$ is associated with carbonate containing apatite ($CO_3HA$) formation on the surface. SEM images demonstrate that the apatite phase covered the entire surface after 30 days immersion in

1.5SBF. These phases consisted of the spheres with diameter of ~0.2 μm.

## References

1. R. Li, A.E. Clark, L.L. Hench, "An investigation of bioactive glass powders by sol-gel processing", *J. Appl. Biomater.*, **2** [4] (1991) 231–239.
2. M.M. Pereira, A.E. Clark, L.L. Hench, "Calcium phosphate formation on sol-gel-derived bioactive glasses in vitro", *J. Biomed. Mater. Res.*, **28** [6] (1994) 693–698.
3. M. Vallet-Regí, A.M. Romero, C.V. Ragel, R.Z. LeGeros, "XRD, SEM-EDS, and FTIR studies of in vitro growth of an apatite-like layer on sol-gel glasses", *J. Biomed. Mater. Res.*, **44** [4] (1999) 416–421.
4. M. Vallet-Regí, I. Izquierdo-Barba, A.J. Salinas, "Influence of $P_2O_5$ on crystallinity of apatite formed in vitro on surface of bioactive glasses", *J. Biomed. Mater. Res.*, **46** [4] (1999) 560–565.
5. M. Vallet-Regi, A. Ramila, "New bioactive glass and changes in porosity during the growth of a carbonate hydroxyapatite layer on glass surfaces", *Chem. Mater.,* **12** (2000) 961–965.
6. A. Balamurugan, G. Balossier, J. Michel, S. Kannan, H. Benhayone, A. Rebelo, J. Fereira, "Sol-gel derived $SiO_2$-CaO-MgO-$P_2O_5$ bioglass system-preparation and in vitro characterization", *J. Biomed. Mater. Res. B: Appl. Biomater.*, **83** (2007) 546–553.
7. V.K. Marghussian, A. Mesgar, "Effects of composition on crystallization behaviour and mechanical properties of bioactive glass-ceramics in the MgO-CaO-$SiO_2$-$P_2O_5$ system", *Ceram. Int.*, **26** [4] (2000) 415–420.
8. A.J. Salinas, J. Román, M. Vallet-Regi, J.M. Oliveira, R.N. Correia, M.H. Fernandes, "In vitro bioactivity of glass and glass-ceramics of the 3CaO·$P_2O_5$-CaO·$SiO_2$-CaO·MgO·2$SiO_2$", *Biomater.*, **21** [3] (2000) 251–257
9. O. Peitl, E. Zanotto, L. Hench, "Highly bioactive $P_2O_5$-$Na_2O$-CaO-$SiO_2$ glass-ceramics", *J. Non-Cryst. Solids*, **292** [1-3] (2001) 115–126.
10. L. Meseguer-Olmo, A. Bernabeu-Esclapez, E. Ros-Martinez, S. Sánchez-Salcedo, S. Padilla, A. I. Martín, M. Vallet-Regí, M. Clavel-Sainz, F. Lopez-Prats, C.L. Meseguer-Ortiz, "In vitro behaviour of adult mesenchymal stem cells seeded on a bioactive glass ceramic in the $SiO_2$-CaO-$P_2O_5$ system", *Acta Biomater.*, **4** [4] (2008) 1104–1113.
11. H-L. Ren, Y. Yue, C.-H. Ye, L-P. Guo, J-H. Lei, "NMR study of crystallization in MgO-CaO-$SiO_2$-$P_2O_5$ glass-ceramics", *Chem. Phys. Lett.*, **292** [3] (1998) 317–322.
12. H. Aguiar, E.L. Solla, J. Serra, P. González, B. León, F. Malz, C. Jäger, "Raman and NMR study of bioactive $Na_2O$-MgO-CaO-$P_2O_5$-$SiO_2$ glasses", *J. Non-Cryst. Solids*, **354** [45-46] (2008) 5004–5008.
13. K. Sharma, S. Singh, C.L. Prajapat, S. Bhattacharya, Jagannath, M.R. Singh, S.M. Yusuf, G.P. Kothiyal, "Preparation and study of magnetic properties of silico phosphate glass and glass-ceramics having iron and zinc oxide", *J. Magn. Magn. Mater.*, **321** [22] (2009) 3821–3828.
14. R.K. Singh, G.P. Kothiyal, A. Srinivasan, "Magnetic and structural properties of CaO-$SiO_2$-$P_2O_5$-$Na_2O$-$Fe_2O_3$ glass ceramics", *J. Magn. Magn. Mater.*, **320** [7] (2008) 1352–1356.
15. D. Eniu, D. Cacaina, M. Coldea, M. Valeanu, S. Simon, "Structural and magnetic properties of CaO-$P_2O_5$-$SiO_2$-$Fe_2O_3$ glass-ceramics for hyperthermia", *J. Magn. Magn. Mater.*, **293** [1] (2005) 310–313.
16. B. Yu, K. Liang, Sh. Gu, "Effect of $ZrO_2$ on crystallization of CaO-$P_2O_5$-$SiO_2$ glasses", *Ceram. Int.*, **28** [6] (2002) 695–698.
17. E. Leonardi, G. Ciapetti, N. Baldini, G. Novajra, E. Verné, F. Baino, C. Vitale-Brovarone, "Response of human bone marrow stromal cells to a resorbable $P_2O_5$-$SiO_2$-CaO-MgO-$Na_2O$-$K_2O$ phosphate glass ceramic for tissue engineering applications", *Acta Biomater.*, in press (2009).
18. G. Li, D. Zhou, Y. Lin, T. Pan, G. Chen, Q. Yin, "Synthesis and characterization of magnetic bioactive glass-ceramics containing Mg ferrite for hyperthermia", *Mater. Sci. Eng. C*, in press (2009).
19. E. Verné, S. Ferraris, C. Vitale-Brovarone, S. Spriano, C. Bianchi, A. Naldoni, M. Morra, C. Cassinelli, "Alkaline phosphatase grafting on bioactive glasses and glass ceramics", *Acta Biomater.*, in press (2009).
20. Z. Hong, A. Liu, L. Chen, X. Chen, X. Jing, "Preparation of bioactive glass ceramic nanoparticles by combination of sol-gel and coprecipitation method", *J. Non-Cryst. Solids*, **355** [6] (2009) 368–372.
21. L. Hench, R. Splinter, W. Allen, T. Greenlee, "Bonding mechanism at the interface of ceramic prosthetic materials", *J. Biomed. Mater. Res. Symp.*, **2** (1971) 117–141.
22. L. Radev, V. Hristov, I. Michailova, B. Samuneva, "Sol-gel bioactive glass-ceramics. Part I: Calcium phosphate silicate/wollastonite glass-ceramics", *Cent. Eur. J. Chem.*, **7** [3] (2009) 317–321.
23. L. Radev, V. Hristov, I. Michailova, B. Samuneva, "Sol-gel bioactive glass-ceramics. Part II: Glass-Ceramics in the CaO-$SiO_2$-$P_2O_5$-MgO system", *Cent. Eur. J. Chem.*, **7** [3] (2009) 322–327.
24. F. Muller, M. Bottino, L. Muller, V. Henriques, U. Lohbauer, A. Bressiani, J. Bressiani, "In vitro apatite formation on chemically treated (P/M) Ti–13Nb–13Zr", *Dental Mater.*, **24** (2008) 50–56.
25. G. Falini, S. Fermani, B. Palazzo, N. Roveri, "Helical domain collagen substrates mineralization in simulated body fluid", *J. Biomed. Mater. Res. A.*, **87** [2] (2008) 470–476.
26. W.G. Mumme, R.J. Hill, G. Bushell-Wye, E.R. Segnit, *N. Jb. Miner. Abh.*, **169** (1995) 35.

27. T. Kanaya, K. Tsuru, S. Hayakawa, A. Osaka, E. Fujii, K. Kawabata, G. Gasqueres, C. Bonhomme, F. Babonneau, "Structure and in vitro solubility of silicon substituted hydroxyapatite", *Key Eng. Mater.*, **361-363** (2008) 63–66.

28. G. Gasquieres, C. Bonhomme, J. Maquet, F. Babonneau, S. Hayakawa, T. Kanaya, A. Osaka, "Revisiting silicate substituted hydroxyapatite by solid-state NMR", *Magn. Reson. Chem.*, **46** (2008) 342–346.

29. Z. Gou, J. Chang, W. Zhai, "Preparation and characterization of novel bioactive dicalcium silicate ceramics", *J. Eur. Ceram. Soc.*, **25** (2005) 1507–1514.

30. M.Y. Benarchid, A. Diouri, A. Boukhari, J. Aride, I. Elkhandiri, "Hydration of iron-phosphorus doped dicalcium silicate phase", *Mater. Chem. Phys.*, **94** (2005) 190–194.

31. Sh. Zou, J. Huang, S. Best, W. Bonfield, "Crystal imperfection studies of pure and silicon substituted hydroxyapatite using Raman and XRD", *J. Mater. Sci.: Mater. Med.*, **16** (2005) 1143–1148.

32. E. S. Thian, J. Huang, M. Vickers, S. Best, Z. Barber, W. Bonfield, "Silicon-substituted hydroxyapatite (SiHA): A novel calcium phosphate coating for biomedical applications", *J. Mater. Sci.*, **41** (2006) 709–714.

33. R. Chrysafi, Th. Perraki, G. Kakali, "Sol-gel preparation of $2CaO.SiO_2$", *J. Eur. Ceram. Soc.*, **27** (2007) 1707–1710.

34. J. Romano, P. Marcato, F. Rodrigues, "Synthesis and characterization of manganese oxide-doped dicalcium silicates obtained from rice hull ash", *Powder Technol.*, **178** (2007) 5–9.

35. V. Jokanović, D. Izvonar, M. D. Dramićanin, B. Jokanović, V. Živojinović, D. Marković, B. Dačić, "Hydrothermal synthesis and nanostructure of carbonated calcium hydroxyapatite", *J. Mater. Sci.: Mater. Med.*, **17** (2006) 539–546.

36. I. Gibson, S. Best, W. Bonfield, "Chemical characterization of silicon-substituted hydroxyapatite", *J. Biomed. Mater. Res.*, **44** (1999) 422–428.

37. J. Anderson, S. Avera, B. Spliethoff, M. Linden, "Sol-gel synthesis of a multifunctional, hierarchically porous silica/apatite composite", *Biomater.*, **26** (2005) 6827–6835.

38. N. Patel, S. Best, W. Bonfield, I. Gibson, K. Hing, E. Damien, P. Revell, "A comparative study on the in vitro behaviour of hydroxyapatite and silicon substityted hydroxyapatite granules", *J. Mater. Sci.: Mater. Med.*, **13** (2002) 1199–1208.

39. M.R. Ahsan, M.G. Mortuza, "Infrared spectra of $xCaO(1-x-z)SiO_2zP_2O_5$ glasses", *J. Non-Cryst. Solids*, **351** (2005) 2333–2340.

40. S.R. Federman, V.C. Costa, D.C. Vasconcelos, W.L. Vasconcelos, "Sol-gel $SiO_2$-$CaO$-$P_2O_5$ biofilm with surface engineered for medical application", *Mater. Res.*, **10** [2] (2007) 177–181.

41. M. Cerruti, D. Greenspan, K. Powers, "Effect of pH ionic strength on the reactivity of Bioglass 45S", *Biomater.*, **26** (2005) 1665–1674.

42. I.R. Gibson, I. Rehman, S.M. Best, W. Bonfield, "Characterization of the transformation from calcium-deficient apatite to β-tricalcium phosphate", *J. Mater. Sci.: Mater. Med.*, **11** [9] (2000) 533–539.

43. I. Rehman, W. Bonfield, "Characterization of hydroxyapatite and carbonated apatite by photo acoustic FTIR spectroscopy", *J. Mater. Sci.: Mater. Med.*, **8** [1] (1997) 1–4.

44. D. Carta, D.M. Pickup, J.C. Knowles, I. Ahmed, M. E. Smith, R.J. Newport, "A structural study of sol-gel and melt-quenched phosphate-based glasses", *J. Non-Cryst. Solids*, **353** (2007) 1759–1765.

45. C.Y. Ooi, M. Hamdi, S. Ramesh, "Properties of hydroxyapatite produced by annealing of bovine bone", *Ceram. Int.*, **33** [7] (2007) 1171–1177.

46. P.N. de Aza, C. santos, A. Pazo, S. de Aza, R. Cusco, L. Artus, "Vibration properties of calcium phosphate compounds. 1. Raman spectrum of beta-tricalcium phosphate", *Chem. Mater.*, **9** (1997) 912–915.

47. P.N. de Aza, F. Guitian, C. Santos, S. de Aza, R. Cusco, L. Artus, "Vibrational properties of calcium phosphate compounds. 2. Comparison between hydroxyapatite and beta-tricalcium phosphate", *Chem. Mater.*, **9** (1997) 916–922.

48. H. Eshtiagh-Hosseini, M.R. Housaindokht, M. Chahkandi, "Effects of parameters of sol-gel process on the phase evolution of sol-gel-derived hydroxyapatite", *Mater. Chem. Phys.*, **106** [2-3] (2007) 310–316.

49. Ch. Su, D. L. Suarez, "In situ infrared speciation of adsorbed carbonate on aluminium and iron oxides", *Clays Clay Minerals*, **45** [6] (1997) 814–825.

50. H. Wijnja, C. Schulthess, "Carbonate adsorption Mechanism on Goethite Studied with ATR-FTIR, DRIFT, and Proton Coadsorption measurements", *Soil Sci. Soc. Am. J.,* **65** (2001) 324–330.

51. Th. Leventouri, C.E. Bunachiu, V. Perdikatsis, "Neutron powder diffraction studies of silicon substituted hdroxyapatite", *Biomater.,* **24** (2003) 4205–4211.

52. B. Boev, G. Jovanovski, P. Makreski, "Minerals from Macedonia. XX. Geological Setting, Lithologies, and Identification of the Minerals from Ržanovo Fe-Ni Deposit", *Turkish J. Earth Sci.*, **18** (2009) 1–22

53. A. Martinez, I. Izquierdo-Barba, M. Vallet-Regi, "Bioactivity of a $CaO$-$SiO_2$ binary glasses system", *Chem. Mater.*, **12** (2000) 3080–3088.

54. M. Zaki, H. Knözinger, B. Tesche, G.A.H. Mekhemer, "Influence of phosphonation and phosphation on surface acid-base and morphological properties of CaO as investigated by in situ FTIR spectroscopy and electron microscopy", *J. Coll. Interface Sci.*, **303** (2006) 9–17.

55. S. Akyuz, T. Akyuz, S. Basaran, I. Kocabas, A. Gulec, H. Cesmeli, B. Ucar, "FT-IR and EDXRF analysis of wall paintings of ancient Ainos Hagia Sophia Church", *J. Molecular Struct.*, **924-926** (2009) 400–403.

56. L-C. Huang, C-C. Lin, P. Shen, "Crystallization and stoichiometry of crystals in $Na_2CaSi_2O_6$-$P_2O_5$ based bioactive glasses", *Mater. Sci. Eng. A,* **452-453** (2007) 326–333.

57. M. Andrés-Vergés, C. Fernández-González, M. Martinez-Gallego, J.D. Solier, I. Cachadiña, E. Matijevic, "A new route for the synthesis of calcium-deficient hydroxyapatites with low Ca/P ratio: Both spectroscopic and electric characterization", *J. Mater. Res.*, **15** [11] (2000) 2526–2533.

58. G. Xu, I. A. Aksay, J.T. Groves, "Continuous crystalline carbonate apatite thin films. A biomimetic approach", *J. Am. Chem. Soc.*, **123** (2001) 2196–2203.

59. J. Li, Y. Li, L. Zhang, Y. Zuo, "Composition of calcium deficient Na-containing carbonate hydroxyapatite modified with Cu(II) and Zn(II) ions", *Appl. Surface Sci.*, **254** (2008) 2844–2850.

60. S. Sprio, A. Tampieri, E. Landi, M. Sandri, S. Martorana, G. Celotti, G. Logroscino, "Physico-chemical properties and solubility behaviour of multi-substituted hydroxyapatite powders containing silicon", *Mater. Sci. Eng. C*, **28** (2008) 179–187.

61. Th. Leventouri, A. Antonakos, A. Kyriacou, R. Venturelli, E. Liarokapis, V. Perdikatsis, "Crystal structure studies of human dental apatite as a function of age", *Int. J. Biomater.*, doi:10.1155/ 2009/698547 (2009).

62. H. El Feki, Ch. Rey, M. Vignoles, "Carbonate ions in apatites: Infrared investigations in the v4 $CO_3$ domain", *Calcified Tissue Int.*, **49** [4] (1991) 269–274.

63. R. Murugan, S. Ramakrishna, K.P. Rao, "Nanoporous hydroxy-carbonate apatite scaffold made of natural bone", *Mater. Lett.*, **60** (2006) 2844–2847.

64. A. Krajewski, A. Ravaglioli, A. Tinti, P. Taddei, M. Mazzocchi, R. Martinetti, C. Fagnano, M. Fini, "Comparison between the in vitro surface transformations of AP40 and RKKP bioactive glasses", *J. Mater. Sci.: Mater. Med.*, **16** (2005) 119–128.

65. L. Radev, V. Hristov, B. Samuneva, D. Ivanova, "Organic/inorganic bioactive materials. Part II: In vitro bioactivity of collagen-calcium phosphate silicate/wollastonite hybrids", *Cent. Eur. J. Chem.*, **7** [4] (2009) 711–720.

66. P. Regnier, A. Lasaga, R. Berner, O. Han, K. Zilm, "Mechanism of $CO_3^{2-}$ substitution in carbonate-fluorapatite: Evidence from FTIR spectroscopy, $^{13}C$ NMR and quantum mechanical calculations", *Am. Mineralogist*, **79** (1994) 809–818.

67. A. Rámila, F. Balas, M. Vallet-Regí, "Synthesis Routes for Bioactive Sol−Gel Glasses: Alkoxides versus Nitrates", *Chem. Mater.*, **14** (2002) 542–548.

68. M. Vallet-Regí, A. Rámila, "New bioactive glass and changes in porosity during the growth of a carbonate hydroxyapatite layer on glass surfaces", *Chem. Mater.*, **12** (2000) 961–965.

69. M.E. Fleet, X. Liu, "Location of type B carbonate ion in type A–B carbonate apatite synthesized at high pressure", *J. Solid State Chem.*, **177** [9] (2004) 3174–3182

70. M. Vallet-Regi, D. Arcos, "Silicon substituted hydroxyapatites. A method for upgrade calcium phosphate based implants", *J. Mater. Chem.*, **15** (2005) 1509–1516.

71. N.Y. Mostafa, H.M. Hassan, F.H. Mohamed, "Sintering behavior and thermal stability of $Na^+$, $SiO_4^{4-}$ and $CO_3^{2-}$ co-substituted hydroxyapatites", *J. Alloys Comp.*, **479** (2009) 692–698.